

## IMPROVING WELD QUALITY WITH OPTIMIZED BOBBIN TOOLS: AN INNOVATIVE APPROACH TO FRICTION STIR WELDING OF ALUMINIUM

Toni Sprigode<sup>1,\*</sup>, Andreas Gester<sup>1</sup>, Guntram Wagner<sup>1</sup>, Angelika Brückner-Foit<sup>2</sup>, Boulbaba Boudhraa<sup>2</sup>, Adrian Rienäcker<sup>2</sup>

<sup>1</sup> Chair of Composites and Material Compounds, Institute of Materials Science and Engineering, Chemnitz University of Technology, 09125 Chemnitz, Germany

<sup>2</sup> University of Kassel, Department of Machine Elements and Tribology, 34125 Kassel, Germany

### ABSTRACT

Friction stir welding (FSW) has gained significant attention as a viable method for joining aluminum alloys due to its ability to produce high-quality welds. In recent years, bobbin tools have emerged as an innovative tool geometry for FSW of aluminum. Because of their unique tool design and weld setup, there is no backing plate needed and weak points such as root defects cannot form. The creation of strong and high-quality joints in similar aluminum structures is a challenging task for welding processes. In this regard, the current study aims at investigating the effect of shape-optimized bobbin tools on the welding quality of the joints. For this purpose, a simulation of the critical run-in process was performed in an initial step. Thus, the contact conditions between the tool and the work-piece could be analyzed, and a qualitative impression was gained of the welding behavior of this welding set-up. Subsequently, the tool was shape-optimized by imposing ideal contact conditions. The optimized and non-optimized tools were then used to perform FSW on similar aluminum joints made of AA5754. The resulting joints were analyzed for their mechanical and microstructural properties, and it was found that the optimized tool led to a different microstructure and tensile strength than the non-optimized tool. Therefore, this study provides a new and effective approach to improve the weld quality of similar aluminum joints by optimizing the geometry of bobbin tools through simulation.

**Index Terms** – Friction Stir Welding, Aluminum, Bobbin Tool, Microstructure, Mechanical Properties, Simulation, Optimization

### 1. INTRODUCTION

Friction Stir Welding (FSW) is a highly advanced welding technique that has gained increasing importance in recent decades. As an innovative approach for creating welded joints, it offers numerous advantages over conventional welding methods. The process is based on the principle of plastic deformation of metals through frictional heat generated during the welding process. It allows for the joining of workpieces without the formation of a melt, leading to a range of positive effects such as low thermal distortion, high weld strength, and excellent reproducibility. In addition, due to the low heat input, joints can be made from similar and dissimilar alloys [1, 2]. This leads to the FSW process being widely used in various industries such as aerospace [3], automotive [4], shipbuilding [5, 6] and even rail vehicle construction [7].



Normally, the joining process is carried out with conventional tools consisting of a shoulder and a probe. The addition of a second shoulder at the lower end of the probe results in a special shape. This unique tool geometry, called the bobbin tool, enables welding over the entire cross-section of the sheets. As a consequence, there are no root defects in the weld seam. Furthermore, the welding setup does not require a backing plate, so that the heat generated by the upper and lower shoulders is completely utilized [8]. Nevertheless, the special tool shape has some challenges. The critical run-in process results in an ejected tail and as the tool moves out of the joining partners, the lack of material results in a keyhole [9].

Aluminum is used as a construction material in many areas due to its numerous advantages. Despite its low weight, aluminum has high strength and is extremely ductile. The mechanical properties can be improved by adding elements such as copper, manganese or silicon. The 5000 series of aluminum alloys contains magnesium as the main alloying element. These alloys cannot be hardened by heat treatment, but still have good strength values. The aluminum alloy AA5754 is used in the automotive industry [10], shipbuilding and civil engineering. Furthermore, this aluminum alloy has an excellent corrosion resistance. AA5754 is preferable to other materials [11] especially in salt water and other aggressive media.

Joining the aluminum alloy AA5754 is possible using various processes like arc welding [12], electric resistance welding [13] or fiber laser welding [14]. However, it has been shown that pressure welding processes are particularly suitable and are characterized by excellent joint strength. In the latest work from Ahmed et al. 2023 [15], a strength of 97 % of the base metal (BM) was achieved when joining 5 mm thick sheets. Parameter variations included the travel speed and the eccentricity of the probe. Another parameter study was carried out by Barlas and Ozsarac 2012 [16]. At constant travel speed, the effects of rotational speed, tilt angle and tool rotation direction were investigated, resulting in a defect free weld with a joint efficiency of 86 %. Furthermore, it is possible to obtain ultimate tensile strengths (UTS) at a level above that of the BM due to well evaluated parameters. Moreover, ultimate tensile strengths (UTS) above that of the BM can be obtained by optimizing the process parameters [17].

In the recent literature, the joint strengths of bobbin tool friction stir welding (BTFSW) of aluminum joints are lower than those of conventional FSW. The review report from Whang et al. 2020 [18] shows that the joint efficiency of BTFSW of 2000 and 6000 aluminum series was in a range between 66 and 83.7 %. Pecanac et al. 2022 [19] investigated the influence of tooling and welding parameters in BTFSW of AA5005 and obtained a joint strength of 83.9 % compared to the BM. However, they detected wormholes in the weld seam, which significantly deteriorate the weld quality. The same observation was made by Balos et al. 2023 [20] who postulated that the occurrence of wormholes decreases with the increase of the welding temperature. A joint efficiency of 97 % was produced by Mardalizadeh et al. 2021 [21] in BTFSW of 20 mm thick AA5456-H112 plates, which is consistent with Marie's 2004 [22] thesis that welding with bobbin tools is more suitable for thick work-pieces than for thinner sheets.

The relationship between process parameters and tool geometry affects material flow and heat generation, which are the most important factors producing high quality welds. For this reason, numerical simulations of the BTFSW process and the tool shape were used to analyze the welding process. Liu et al. 2013 [23] simulated the joining process of 6 mm AA2014 sheets and calculated that the peak temperature on the advancing side (AS) is about 40 °C lower than that of the retreating side (RS). Wen et al. 2018 [24] localized the peak temperature at the center of the cross-section of the weld seam using a numerical simulation of the BTFSW process of a 4 mm thick AA2219-T87 piece. Simulations of the material velocity show the typical hourglass shape that is well-known from microstructure analysis of the joint. This is caused by the higher flow velocity of the material at the shoulders and the lower velocity around the probe [24, 25]. Furthermore, even defects could be exposed. Fraser et al. 2014 [26] show that a tail is created

while the tool runs into the sheet which leads to a non-welding region. Additionally, a blow-out hole is created while running out.

In this study, a numerical simulation of the BTFSW process was performed in order to study the run-in process. Interest was focused on the temperature distribution and the contact conditions between the tool and the work-piece. Based on these results for a standard tool geometry, a shape-optimized tool was defined with the side condition of constant normal stresses on the tool. BTFSW experiments were performed with both the standard bobbin tool and the optimized tool, and the welding results are compared with each other.

## 2. MATERIALS AND METHODS

The work-pieces were cut from sheet material of the aluminum alloy AA5754-H111, and had dimensions of 140 x 100 x 4 mm. The chemical composition and mechanical properties of the base material are listed in Table 1. The material was in an H111 heat-treated state. i.e. is annealed and additionally slightly work-hardened. The work-pieces were clamped in all directions to ensure reliable welding (Figure 1b).

**Table 1: Chemical composition and mechanical properties of AA5754**

Material	Elements									R <sub>p0.2</sub> MPa	R <sub>m</sub> MPa
	Si	Fe	Cu	Mn	Mg	Cr	Zn	Ti	Al		
AA5754	0.4	0.4	0.1	0.5	2.6 - 3.6	0.3	0.2	0.15	Bal.	88	213

FSW experiments were performed on a four-axis universal machining center DMU80T from DMG Mori (Wernau, Germany) with a travel speed of 12,5 mm/min and a rotational speed of 4500 1/min with counterclockwise rotation. The dimensions of the original, non-optimized bobbin tool are shown in Figure 1a. The tool is made of AISI H13 tool steel. In addition, thermocouples of type K were placed 10 mm on AS and RS on the lower and upper side and one between the sheets at a distance of 100 mm from the start of welding in order to investigate the temperature distribution during welding. After welding, the joints were examined mechanically and microstructurally. For this purpose, the tensile testing machine ProLine from ZwickRoell (Ulm, Germany) with a load cell of 10 kN was used. The testing speed of the tensile tests was 2.5E-3 1/s. Light microscopic images of the cross-sections of the welds were taken

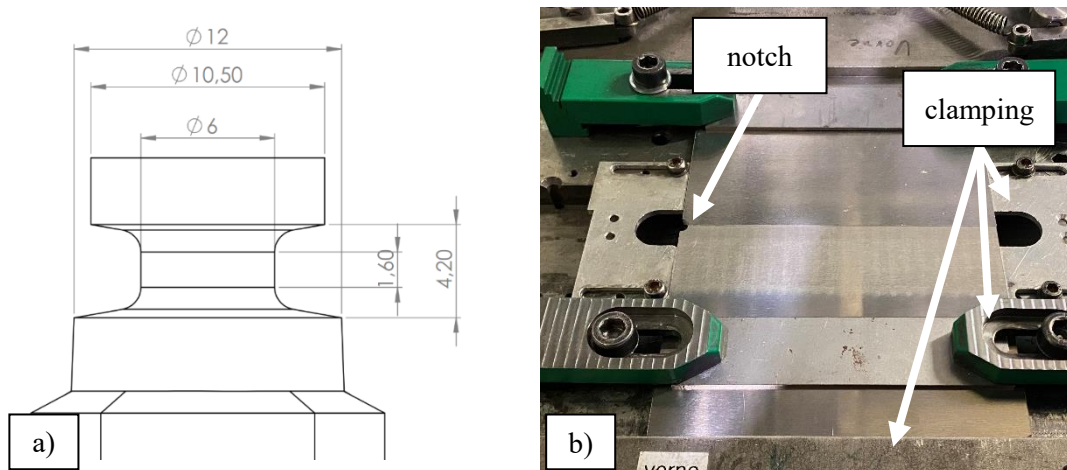


**Figure 1: (a) Dimensions of the non-optimized bobbin tool, (b) welding setup**

with an Olympus GX51 from Zeiss (Jena, Germany) after the samples had been etched with 5% HF according to Flick's method.

The run-in of the BTFSW process corresponding to the first 10mm of the weld seam was simulated as a forming process using the simufact forming code (simufact engineering, Hamburg, Germany). As there is no option for material mixing in the code, the work-piece was modelled as a single sheet. Material transport occurred due to friction (friction coefficient of 0.7). In the forming process, material can stick to the tool with separation occurring at deformation induced stresses levels exceeding the separation strength. The separation strength was varied in the range of 0 and 50 MPa with the upper limit given by the strength of the base material at maximum temperature.

The simulation starts with the tool rotating in contact to the work piece in order to reach a minimum temperature, which is required for achieving material transport. The work-piece was pre-heated to 150°C in order to reduce simulation time. Then the tool starts to advance in welding direction at a constant travelling speed. Material is transported to the backside of the tool by plastic deformation induced both by tool advance and tool rotation, and the gap behind the tool is partially filled. "Good" welding conditions are characterized by a small remaining gap in the rear-side of the tool, see e.g. Figure 2b.

The simulation yields time-dependent deformation and temperature fields in various forms together with contact conditions. Tool loading during the forming process can be calculated explicitly or estimated in terms of the stresses acting in the area of maximum contact (see figure 2). Tool loading, in turn, can be used as a basis for tool optimization using the topology optimization tool TOSCA (Topology Optimization Using Stress Constrains and Adaptive Meshing) from Simulia (Johnston, USA). Genuine topological volume optimization reduces the total mass of a given component while maintaining its load bearing capacity. Shape optimization, on the other hand, aims at reducing stresses in the design region by varying the contour of the component. Shape optimization is used in the following in order to improve the welding behavior of the bobbin tool.

### 3. RESULTS

#### 3.1 Run-in process

The initial simulation runs of the run-in process revealed high plastic deformation of the work-pieces, low temperatures in the contact region, and an insufficient material flow. This is the result of the poor contact conditions between the tool and the aluminum sheet (Figure 2a). To avoid this, a semicircular notch was introduced at the run-in side of the work-piece with the diameter of the probe. The result is that material transport starts with the beginning of tool

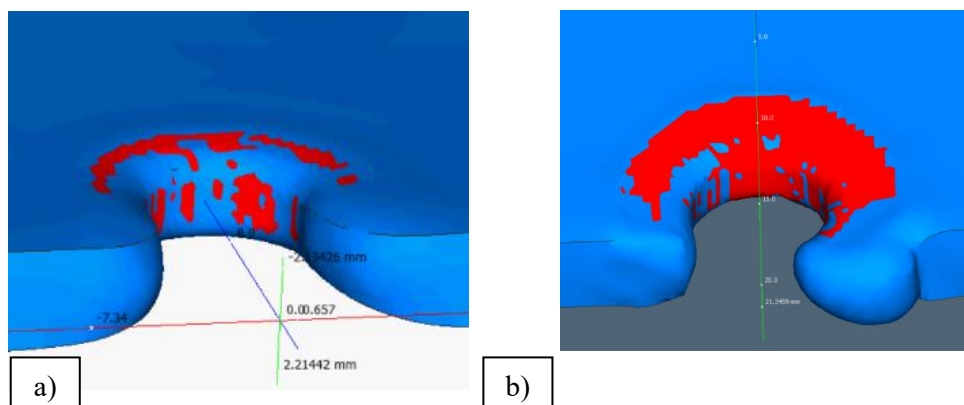


**Figure 2: Contact conditions between tool shoulders and sheet (a) without a notch and (b) with a notch; full contact: red, no contact: blue**

advance. This is reflected in the contact conditions shown in Figure 2. This initial notch was also used in the welding experiments (see Figure 1b).

### 3.2 Shape optimization

In general, shape optimization is used to reduce local stress concentrations. This aspect is relevant in case of the bobbin tool, as high local loading will induced higher wear rates and consequently lower lifetimes of the tool. Moreover, it was found in the simulations of the BTFSW process that regions of good contact are characterized by constant values of the von Mises stress. This fact gave rise to the idea that an ideal tool should impose constant normal stresses throughout the region of contact, and hence, it should be shape-optimized with the boundary condition that constant normal stresses are acting along the shoulders and the probe. For this purpose, a two-domain axisymmetric mesh was set-up for the tool shown in figure 1a, with an variable contour layer for shape optimization. Normal stresses of 100 MPa are then imposed on the surfaces of the shoulders and the probe, and a shape optimization is performed using TOSCA.

Figure 3 shows the stress distribution on the tool surface before and after optimization. The original tool design leads to rather pronounced stress concentrations in the transition region between shoulders and probe with maximum stress enhancement factor of 4.75 whereas the maximum principal stress attains a maximum value of 344 MPa in the optimized case, i.e. the maximum stress intensity factor amounts to 3.44.

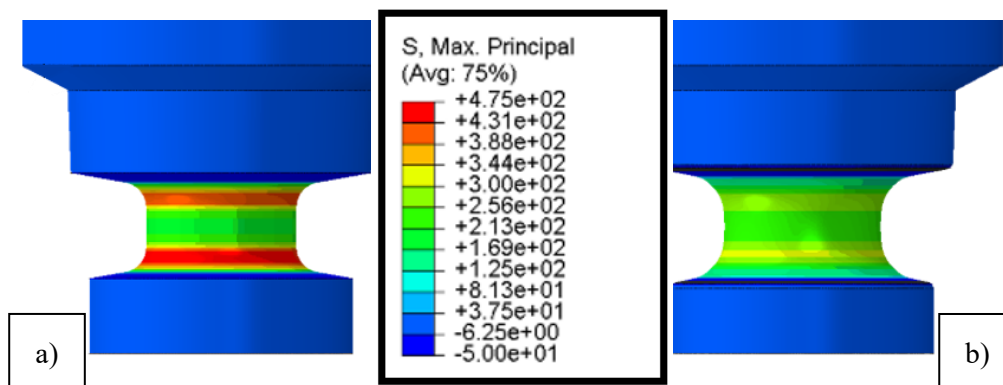


Figure 3: Stress distribution in the bobbin tool subjected to a normal surface stress of 100 MPa (a) before shape optimization and (b) after shape optimization

### 3.3 Welding process

BTFSW was performed with AA5754 sheets with optimized and non-optimized tools. In both cases, solid joints were formed. When welding with the non-optimized tool, however, a wormhole was formed over the entire weld seam on the lower side of the sheet. An ejected tail was found on RS (Figure 4b) during run-in until complete stirring, and a keyhole occurred at

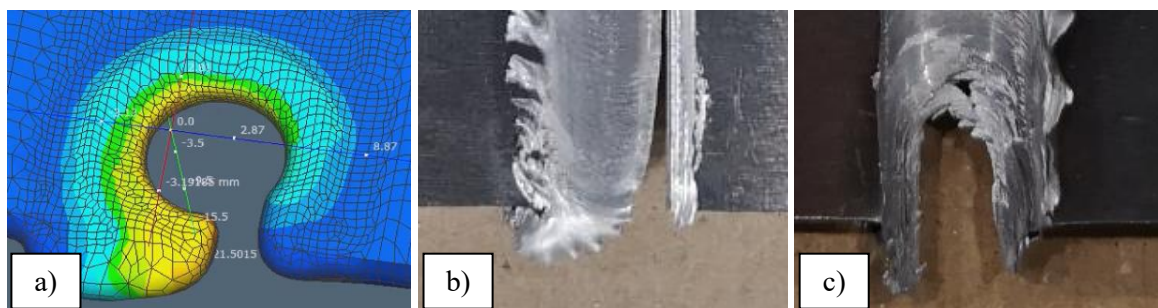
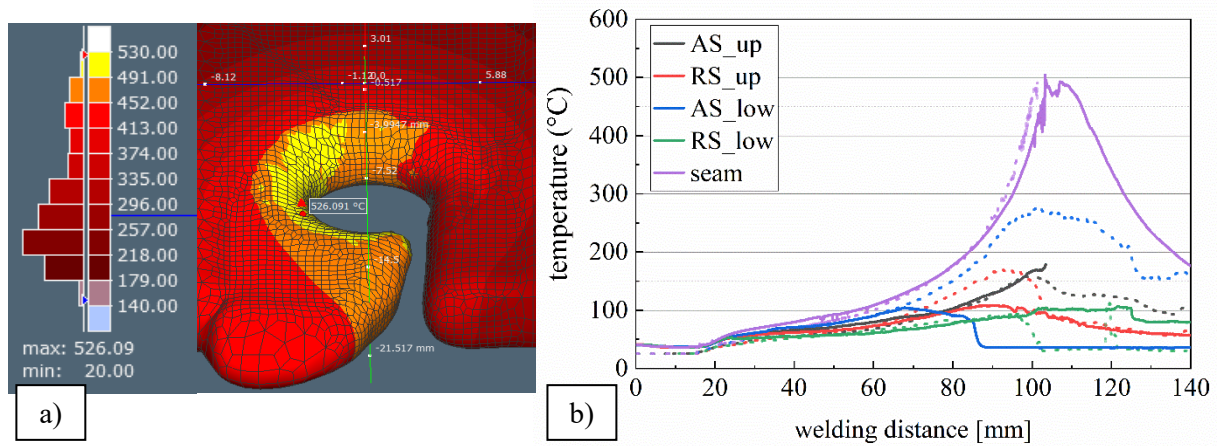


Figure 4: Ejected tail (a) in the simulation and (b) in the experiment; (c) key-hole defect



the end of the weld seam (Figure 4c), because the moving tool pushes the material out of the sheets and no stirring is possible. These two defects are in agreement with the current literature [9, 26] and are typical for welding with bobbin tools. An ejected tail was also found in the simulation of the BTFSW process (Figure 4a). Changing process parameters strongly affects the conditions also the predicted form the ejected tail. This fact will be used in future improvements of the BTFSW process.



**Figure 5: (a) Simulated temperature distributions during BTFSW with optimized bobbin tool, (b) temperature distributions during BTFSW - thermocouples placed at 100 mm; dotted line: non-optimized tool, continuous line: optimized tool**

Figure 5a summarizes the results of the temperature measurements with the thermocouples. The peak temperature in the weld seam is above 450°C both for the original bobbin tool and for the shape-optimized one, with peak values approaching 500°C. Minor differences in the peak values can be attributed to the discretization error in the case of the simulation and the measurement error in the experiment, which increase when the tool is approaching. A certain asymmetry in the temperature distribution was observed in the experiments the originally designed bobbin tool (blue and red dotted lines in Figure 5b). Apparently, a certain amount of the generated heat was dissipated in regions of the work-piece lying outside the weld seam region. This effect was also observed in simulation of the BTFSW process, and can be explained by the fact that significant plastic deformation occurs outside the welding zone, when contact between the tool and the work-piece is lost.

### 3.4 Tensile tests

Tensile tests performed with the originally designed bobbin tool have a strength of 55.6 MPa. This is significantly below the strength of the base metal (218.6 MPa) and indicates that the unoptimized tool was not able to produce a sufficiently strong joint. In contrast, strength values of 135.8 MPa (62.1 % compared to the base metal) were obtained with the shape optimized tool. Although this strength is still below that of the base material, it shows a significant improvement compared to the originally designed tool. The optimization of the tool obviously resulted in better material mixing and a stronger weld in agreement with the performance of both tools in the simulation. It should be noted that the strength of the welded joints also depends on the process parameters, which were not optimized in this study. However, the results obtained are encouraging and clearly indicate that shape optimization of the tool is a viable way to improve the weld quality in the BTFSW process.

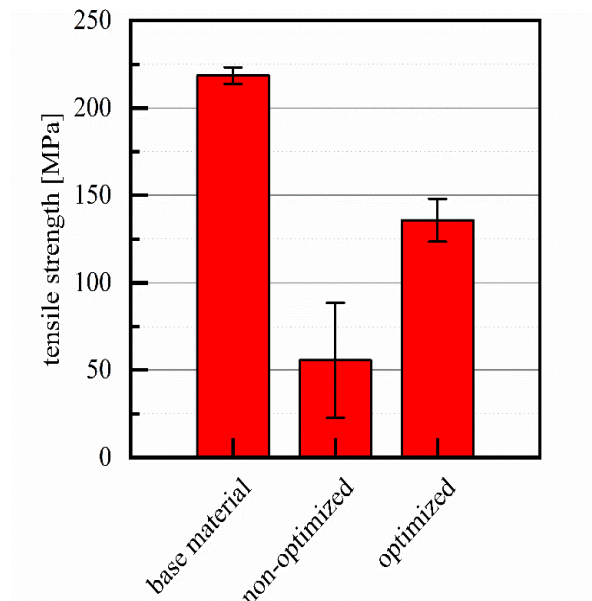


**Figure 6: Tensile strengths [MPa] of base material and joints welded with non-optimized and optimized tool**

### 3.5 Microstructure

The light microscope images of the microstructure of friction stir welded aluminum joints (Figure 7) produced with optimized and non-optimized bobbin tools provide important insights

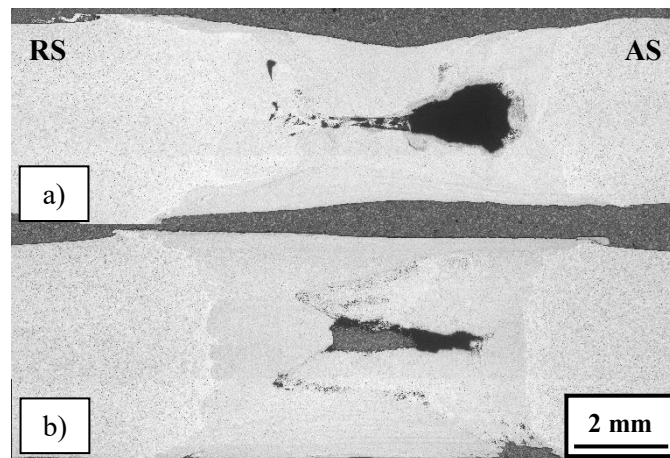


**Figure 7: Light microscopy images of welds using (a) originally designed and (b) shape-optimized tool**

into the quality of the welded joints. Both images show the hourglass shape typical of bobbin tools, which is generated by the rotation of the tool, the feed along the welding direction and the unique tool shape. In both micrographs, tunnel defects are visible in the center of the stirred zone, although the size of these defects is smaller when the shape-optimized tool is used. Since the tunnel defect of the weld of the shape-optimized tool is fairly elongated, it has less influence on the tensile strength, as the loading direction of the tensile test is perpendicular to the weld and hence parallel to the tunnel defect. A clear and pronounced transition between the heat-affected zone and the stirred zone can be seen on both sides of the weld in the case of the shape-optimized tool. In contrast, the transition between the heat-affected zone and the stirring zone is less pronounced on RS for the originally designed tool. This indicates non-uniform material mixing or less stable welding conditions.

In summary, the microstructural analysis implies that the shape-optimized tool geometry and the corresponding process parameters lead to improved material mixing. This is in agreement with the findings of the BTFSW simulation. Here, the minimum gap between the material flanks on the rear side can be taken as an heuristic criterion for material mixing, and the values obtained are 2.03mm for the standard tool, and 1.11mm for the shape-optimized tool, respectively (see figure 8).

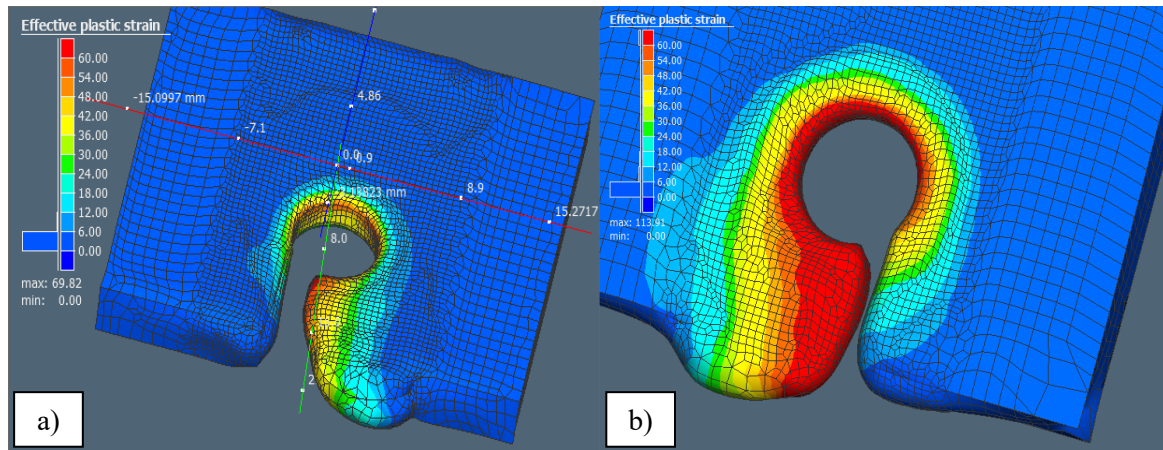


**Figure 8: Results of welding simulation a) with standard bobbin tool (clockwise turning) b) with shape-optimized tool (counterclockwise turning)**

#### 4. CONCLUSION

In the present work, simulation and experimental studies were carried out of BTFSW of AA5754 aluminum sheets with both a classical bobbin tool and a shape-optimized bobbin tools. The main findings can be summarized as follows:

- The simulation of the run-in process shows that the introduction of a notch with the diameter of the probe improves the contact between the shoulder and the aluminum sheet.
- Shape optimization of the bobbin tool reduces the bending stresses at the transition between the probe and the shoulder by over 27 %.
- Solid joints were made with both tool geometries. However, defects such as an ejected end and a keyhole occurred.
- The strength of the welds with the optimized tool is 135.8 MPa, while with the non-optimized tool it is only 55.6 MPa. This is due to more pronounced wormholes when using the classical tool.
- The results show that the shape-optimization of the bobbin tool leads to improved welds. Further optimization in terms of process parameters could lead to higher strength values.

#### CONTACTS

Toni Sprigode, M.Sc.

email: [toni.sprigode@mb.tu-chemnitz.de](mailto:toni.sprigode@mb.tu-chemnitz.de)

ORCID: <https://orcid.org/0000-0001-6295-5441>

#### 5. REFERENCES



- [1] R. K. Bhushan, and D. Sharma: Green welding for various similar and dissimilar metals and alloys : Present status and future possibilities. In: *Advanced Composites and Hybrid Materials 2* (2019), Nr. 3, S. 389–406. URL <http://dx.doi.org/10.1007/s42114-019-00094-8>
- [2] L. E. Murr: A Review of FSW Research on Dissimilar Metal and Alloy Systems. In: *Journal of Materials Engineering and Performance* 19 (2010), Nr. 8, S. 1071–1089
- [3] M. M. Z. Ahmed, M. M. El-Sayed Seleman, D. Fydrych, and G. Çam: Friction Stir Welding of Aluminum in the Aerospace Industry : The Current Progress and State-of-the-Art Review. In: *Materials* 16 (2023), Nr. 8, S. 2971. URL <http://dx.doi.org/10.3390/ma16082971>
- [4] O. Kayode, and E. T. Akinlabi: An overview on joining of aluminium and magnesium alloys using friction stir welding (FSW) for automotive lightweight applications. In: *Materials Research Express* 6 (2019), Nr. 11, S. 112005. URL <http://dx.doi.org/10.1088/2053-1591/ab3262>
- [5] K. Dudzik, and M. Czechowski: Analysis of possible shipbuilding application of friction stir welding (FSW) method to joining elements made of AlZn5Mg1 alloy. In: *Polish Maritime Research* 16 (2009), Nr. 4, S. 38–40
- [6] J. Beaudet, G. Rückert, and F. Cortial: Fatigue behavior of FSW high-yield strength steel welds for shipbuilding application. In: *Welding in the World* 63 (2019), Nr. 5, S. 1369–1378. URL <https://link.springer.com/article/10.1007/s40194-019-00750-z>
- [7] T. KAWASAKI, T. MAKINO, K. MASAI, H. OHBA, Y. INA, and M. EZUMI: Application of Friction Stir Welding to Construction of Railway Vehicles. In: *JSME International Journal Series A* 47 (2004), Nr. 3, S. 502–511. URL <http://dx.doi.org/10.1299/jsmea.47.502>
- [8] K. Fuse, and V. Badheka: Bobbin tool friction stir welding : A review. In: *Science and Technology of Welding and Joining* 24 (2019), Nr. 4, S. 277–304
- [9] M. M. Z. Ahmed, M. I. A. Habba, M. M. El-Sayed Seleman, K. Hajlaoui, S. Ataya, F. H. Latief, and A. E. El-Nikhaily: Bobbin Tool Friction Stir Welding of Aluminum Thick Lap Joints : Effect of Process Parameters on Temperature Distribution and Joints' Properties. In: *Materials* 14 (2021), Nr. 16
- [10] F. Gabrielli, A. Forcellese, M. E. Mehtedi, and M. Simoncini: Mechanical Properties and Formability of Cold Rolled Friction Stir Welded Sheets in AA5754 for Automotive Applications. In: *Procedia Engineering* 183 (2017), S. 245–250. URL <https://www.sciencedirect.com/science/article/pii/S1877705817315357>
- [11] M. Trueba, and S. P. Trasatti: Study of Al alloy corrosion in neutral NaCl by the pitting scan technique. In: *Materials Chemistry and Physics* 121 (2010), Nr. 3, S. 523–533. URL <https://www.sciencedirect.com/science/article/pii/S0254058410001033>
- [12] A. Liu, X. Tang, and F. Lu: Study on welding process and prosperities of AA5754 Al-alloy welded by double pulsed gas metal arc welding. In: *Materials & Design* 50 (2013), S. 149–155
- [13] Y. Bi, Z. Luo, J. Guo, Y. Yang, J. Su, and Y. Zhang: Joint formation mechanism and performance of resistance butt spot welding for AA 5754 aluminum alloy sheet. In: *Materials Letters* 319 (2022), 1–2, S. 132279
- [14] M. Garavaglia, A. G. Demir, S. Zarini, B. M. Victor, and B. Previtali: Fiber laser welding of AA 5754 in the double lap-joint configuration : Process development, mechanical

- characterization, and monitoring. In: *The International Journal of Advanced Manufacturing Technology* 111 (2020), 5-6, S. 1643–1657
- [15] M. M. Z. Ahmed, A. R. S. Essa, S. Ataya, M. M. El-Sayed Seleman, A. A. El-Aty, B. Alzahrani, K. Touileb, A. Bakkar, J. J. Ponnore, and A. Y. A. Mohamed: Friction Stir Welding of AA5754-H24 : Impact of Tool Pin Eccentricity and Welding Speed on Grain Structure, Crystallographic Texture, and Mechanical Properties. In: *Materials* 16 (2023), Nr. 5
- [16] Z. Barlas, and U. Ozsarac: Effects of FSW Parameters on Joint Properties of AlMg3 Alloy. In: *American Welding Society* (2012). URL [https://app.aws.org/wj/supplement/WJ\\_2012\\_01\\_s16.pdf](https://app.aws.org/wj/supplement/WJ_2012_01_s16.pdf)
- [17] L. A. C. de Filippis, L. M. Serio, D. Palumbo, R. de Finis, and U. Galietti: Optimization and Characterization of the Friction Stir Welded Sheets of AA 5754-H111 : Monitoring of the Quality of Joints with Thermographic Techniques. In: *Materials* 10 (2017), Nr. 10
- [18] G.-Q. Wang, Y.-H. Zhao, and Y.-Y. Tang: Research Progress of Bobbin Tool Friction Stir Welding of Aluminum Alloys : A Review. In: *Acta Metallurgica Sinica (English Letters)* 33 (2020), Nr. 1, S. 13–29
- [19] M. Pecanac, D. L. Zlatanovic, N. Kulundzic, M. Dramicanin, Z. Lanc, M. Hadzistević, S. Radisic, and S. Balos: Influence of Tool and Welding Parameters on the Risk of Wormhole Defect in Aluminum Magnesium Alloy Welded by Bobbin Tool FSW. In: *Metals* 12 (2022), Nr. 6, S. 969
- [20] S. Balos, D. Labus Zlatanovic, N. Kulundzic, P. Janjatovic, M. Dramicanin, Z. Lanc, M. Hadzistevic, S. Radisic, D. Rajnovic, and M. Pecanac: Influence of Tool-base Metal Interference on the Performance of Aluminum-Magnesium Alloy Joined by Bobbin Tool Friction Stir Welding, 2023
- [21] M. Mardalizadeh, M. Khandaei, and M. A. Safarkhanian: Influence of travel speed on the microstructural evaluation and mechanical characteristics of bobbin tool friction stir-welded thick AA5456-H112 plates. In: *Journal of Adhesion Science and Technology* 35 (2021), Nr. 1, S. 90–109
- [22] MARIE, F. (Hrsg.); ALLEHAUX, D. (Hrsg.); ESMILLER, B. (Hrsg.): *Development of the Bobbin Tool Technique on Various Aluminum Alloys* : TWI, 2004
- [23] X. M. Liu, J. S. Yao, Y. Cai, H. Meng, and Z. D. Zou: Simulation on the Temperature Field of Bobbin Tool Friction Stir Welding of AA 2014 Aluminium Alloy. In: *Applied Mechanics and Materials* 433-435 (2013), S. 2091–2095
- [24] Q. Wen, W. Y. Li, Y. J. Gao, J. Yang, and F. F. Wang: Numerical simulation and experimental investigation of band patterns in bobbin tool friction stir welding of aluminum alloy. In: *The International Journal of Advanced Manufacturing Technology* 100 (2019), 9-12, S. 2679–2687
- [25] S. J. Chen, A. L. Lu, D. L. Yang, S. Lu, J. H. Dong, and C. L. Dong: Analysis on flow pattern of bobbin tool friction stir welding for 6082 aluminum. In: FUJII, H. (Hrsg.): *Proceedings of the 1st International Joint Symposium on Joining and Welding* : Osaka, Japan, 6-8 November 2013. Cambridge : Woodhead, 2013, S. 353–358
- [26] K. Fraser, L. St-Georges, and L. I. Kiss: *Numerical-Simulation-of-Bobbin-Tool-Friction-Stir-Welding* (2014). URL [https://www.researchgate.net/profile/Kirk-Fraser/publication/275271390\\_Numerical\\_Simulation\\_of\\_Bobbin\\_Tool\\_Friction\\_Stir\\_W](https://www.researchgate.net/profile/Kirk-Fraser/publication/275271390_Numerical_Simulation_of_Bobbin_Tool_Friction_Stir_W)

elding/links/553653070cf218056e93ccda/Numerical-Simulation-of-Bobbin-Tool-Friction-Stir-Welding.pdf